

Bose-Einstein condensation in solid ^4He

D. E. Galli, M. Rossi, and L. Reatto

INFN and Dipartimento di Fisica, Università degli Studi di Milano, Via Celoria 16, 20133 Milano, Italy

(Received 30 September 2004; published 20 April 2005)

We have computed the one-body density matrix ρ_1 in solid ^4He at $T=0$ K using the shadow wave-function (SWF) variational technique. The accuracy of the SWF has been tested with an exact projector method. We find that off-diagonal long-range order is present in ρ_1 for a perfect hcp and bcc solid ^4He for a range of densities above the melting one, at least up to 54 bars. This is first microscopic indication that Bose Einstein condensation (BEC) is present in perfect solid ^4He . At melting, the condensate fraction in the hcp solid is 5×10^{-6} and it decreases by increasing the density. The key process giving rise to BEC is the formation of vacancy interstitial pairs. We also present values for Leggett's upper bound on the superfluid fraction deduced from the exact local density.

DOI: 10.1103/PhysRevB.71.140506

PACS number(s): 67.80.-s

The supersolid state, a solid with superfluid properties, is moving out from theoretical speculations as a result of the observation of nonclassical rotational inertia (NCRI) in solid ^4He in Vycor¹ and very recently in the bulk.² The initial theoretical suggestion^{3,4} of the supersolid state was based on the possible presence of vacancies in the ground state of a Bose quantum solid. In addition, these vacancies have to be mobile in order to give rise to Bose Einstein condensation (BEC) of ^4He atoms. Experimentally, no evidence has been found for the presence of vacancies at very low temperature and this is in agreement with the results of microscopic theory,^{5,6} which gives an energetic cost of about 15 K for the formation of a vacancy in bulk solid ^4He . However, it was almost immediately recognized⁷ that the presence of ground-state vacancies is only one possible mechanism for NCRI, and what is really needed is that atoms are not localized at the lattice sites but are delocalized via exchange or other processes. This gives the possibility of having in the wave function (wf) a phase which governs collectively the motion of the atoms. The existence of a supersolid state in ^4He is therefore strictly related to the question of localization or delocalization of particles and, of course, this is a topic of general interest. This is the case, for instance, of cold alkali atoms in a periodic potential.⁸ Experiments with ^4He give access to the superfluid fraction ρ_s/ρ which turns out to be² at most of order 2%. Theoretically, only upper bounds on ρ_s have been obtained up to now⁹⁻¹¹ and no microscopic theory has given evidence for a supersolid phase. The commonly accepted view is that one can have a finite ρ_s in a three-dimensional system if there is BEC in the system, so a central quantity to compute is the off-diagonal one-body density matrix $\rho_1(\vec{r}, \vec{r}')$, whose Fourier transform represents the momentum distribution.

In this article we address the computation of ρ_1 for solid ^4He at $T=0$ K based on a variational wf, a shadow wf (SWF). In a previous computation¹² we have found that the presence of vacancies in the solid induces a BEC which is proportional to the concentration of vacancies. On the other hand, the large energy of formation of a vacancy makes the probability of having such defects at low temperature vanishingly small. Here we study in the perfect solid the large

distance behavior of $\rho_1(\vec{r}, \vec{r}')$, specifically if ρ_1 has a nonzero limit at large distance (off-diagonal long-range order, ODLRO) which implies BEC. With perfect solid we mean that the number of maxima in the local density $\rho(\vec{r})$ is equal to the number of ^4He atoms. The use of SWF is especially useful in the present context because with such wf the crystalline order is an effect of the spontaneously broken symmetry so that local disorder processes such as the exchange of two or more particles, creation of vacancy interstitial pairs (VIP), or more complex processes are in principle allowed. The major finding of our computation is the presence of a small but finite condensate for a range of densities above melting. The variational theory is very useful to describe strongly interacting systems, such as liquid or solid ^4He , but it is always open to debate how much the results depend on the ansatz on the wf, especially for quantities other than the energy. In order to give an indication on the reliability of our SWF we present some results on quantities including the degree of local order, of localization, and of the local density obtained also from an exact computation¹³ based on the projection algorithm SPIGS, a path integral ground-state method¹⁴ which uses a SWF as the starting wf.

In a SWF the correlations between atoms are introduced both explicitly by a Jastrow factor and also in an implicit way by coupling with a set of subsidiary variables, called "shadow" variables¹⁵ (one shadow for each quantum particle), which are integrated over. All expectation values are computed by a Monte Carlo (MC) method and the statistical sampling of $|\Psi|^2$ maps the quantum system of N particles in a system of N special interacting triatomic "molecules"¹⁵ which consist of a ^4He atom and two shadows. The accuracy of the SWF technique is well documented and it has been possible to treat also disorder phenomena in a quantum solid, i.e., a vacancy^{5,6} or even the interfacial region between a solid and a liquid at coexistence.¹⁶ As a functional form for the correlating factors contained in the SWF we have taken the ones used in Ref. 5; as interatomic interaction we have used a standard Aziz potential.¹⁷

A SWF can be interpreted as a first projection step in imaginary time of a Jastrow wf via a variationally optimized imaginary time propagator.¹³ With SPIGS one goes beyond

TABLE I. Upper bounds f_s^+ for the superfluid fraction in hcp bulk solid ^4He computed at different densities with the SWF technique, the SPIGS method, and the GM for $\rho(\vec{r})$. P is the pressure from the SPIGS equation of state. σ is the standard deviation of the Gaussians used in the GM.

ρ (\AA^{-3})	P (bar)	SWF f_s^+	SPIGS f_s^+	GM f_s^+	σ (\AA)
0.0290	29.3	0.287	0.384	0.380	0.543
0.0310	53.6	0.255	0.299	0.297	0.503
0.0330	87.8	0.209	0.230	0.222	0.467
0.0353	141.9	0.141	0.164	0.166	0.436
0.0400	316.9	0.077	0.080	0.079	0.381
0.0440	553.5	0.042	0.042	0.041	0.345

the variational theory by adding successive projection steps in the imaginary time propagation with the full Hamiltonian and in this way we are able to compute exact expectation values on the ground state without extrapolations. With these two quantum MC methods, no *a priori* equilibrium positions for the solid phase are required, the Bose symmetry is manifestly maintained, and atoms can be delocalized.

The equation of state given by SWF is in good agreement with the results of SPIGS; for instance, at melting ($\rho = 0.029 \text{\AA}^{-3}$) the energy per particle is -5.12 K , 0.76 K above the SPIGS result.¹⁸ Also for a vacancy there is an excellent agreement; the formation energy at melting is 15.7 K with SPIGS and 15.6 K with SWF (Ref. 6) and the jumping rate is similar in the two computations. In addition to the energy one would like to know the accuracy of SWF in describing the microscopic local processes and to this end we have computed the local density $\rho(\vec{r})$ and the static structure factor $S(\vec{k})$. We find again agreement between SWF and SPIGS with SWF giving a slightly more ordered state. For instance, at melting, the main Bragg peak of the hcp solid is about 17% higher than the SPIGS result. A detailed comparison will be presented elsewhere and here we focus only on the results for the upper bound f_s^+ for the superfluid fraction ρ_s/ρ obtained by Leggett.⁷ This bound depends on the averaged density, $\rho(z) = \int d\xi \rho(\vec{r})$, where z is a longitudinal coordinate and ξ is a suitable set of transversal coordinates.⁷ We have chosen as z axis the one which gives the lowest value of f_s^+ ; in the hcp crystal this is the ΓA direction which is perpendicular to the basal plane. It should be noticed that usually in quantum MC computations the center of mass of the system is not fixed and this would alter the local density especially around the minima. Therefore, when we compute $\rho(\vec{r})$ we have modified the sampling algorithm to keep the center of mass of the system fixed. In Table I we show the upper bounds, f_s^+ , for the superfluid fraction obtained for hcp bulk solid ^4He with the SPIGS and SWF methods. There is a substantial agreement, with the variational f_s^+ being always lower as a consequence of the larger degree of local order. A popular representation of $\rho(\vec{r})$ is the one in terms of a sum of Gaussians centered on the lattice sites. We have fitted our $\rho(\vec{r})$ with this Gaussian model (GM) by using the standard

deviation σ as a fitting parameter. We find that the GM gives an excellent representation of the integrated density along planes—what is needed in the Leggett’s inequality—the deviation being below 4%. The resulting bounds given by GM with σ fitted on the SPIGS $\rho(\vec{r})$ are also shown in Table I. The bound f_s^+ given by SWF is similar to the value computed previously⁹ with the GM fitted on a different variational theory. In Refs. 10 and 11 a lower f_s^+ has been obtained by using a better variational ansatz: the phase of the wf is a function of \vec{r} and not only of the longitudinal coordinate z as in Ref. 7. This bound computed with the GM for a given crystal lattice is simply a function of the “localization parameter.”^{10,11} Saslow’s computation is for an fcc crystal but if we neglect the difference between the hcp and the fcc lattice, using the σ in Table I and the results in Ref. 11, we can estimate an f_s^+ which goes from about 0.2 at $\rho = 0.029 \text{\AA}^{-3}$ to about 0.005 at $\rho = 0.044 \text{\AA}^{-3}$. A SPIGS computation for fcc at $\rho = 0.029 \text{\AA}^{-3}$ gives a σ in the GM which is only 2% lower than in hcp crystal. These values of f_s^+ are compatible with the experiments but f_s^+ is about one order of magnitude larger than the experimental value of ρ_s/ρ and, in any case, it is only an upper bound so it is not very conclusive. A word of caution on the GM is in order. If this model gives an excellent representation for the integrated density $\rho(z)$, the accuracy is lost when we consider the local density $\rho(\vec{r})$: in the region of the minima of $\rho(\vec{r})$ deviations greater than 100% are found.

The one-body density matrix $\rho_1(\vec{r}, \vec{r}')$ is given by the overlap between the normalized many-body ground-state wf $\Psi(R)$ and $\Psi(R')$ where configuration $R' = \{\vec{r}', \vec{r}_2, \dots, \vec{r}_N\}$ differs from $R = \{\vec{r}, \vec{r}_2, \dots, \vec{r}_N\}$ only by the position of one of the N atoms in the system; if $\Psi(R)$ is translationally invariant, as in our case when the center of mass is not fixed, ρ_1 only depends on the difference $\vec{r} - \vec{r}'$,

$$\rho_1(\vec{r} - \vec{r}') = N \int d\vec{r}_2 \dots d\vec{r}_N \Psi^*(R) \Psi(R'). \quad (1)$$

It is possible to interpret the integrand in Eq. (1) as a probability density;¹² then ρ_1 can be computed by sampling the integrand in Eq. (1) and by histogramming the occurrence of the distance $\vec{d} = \vec{r} - \vec{r}'$. In the following we will call “half” particles the particles with coordinates \vec{r} and \vec{r}' because they have just $\frac{1}{2}$ the correlation strength with the other $N-1$ particles (with coordinates $\{\vec{r}_2, \dots, \vec{r}_N\}$) and no direct correlation between them. The method of computation has been described in Ref. 12. The absence of ODLRO corresponds to the two “half” particles forming a “molecule,” whereas the presence of ODLRO corresponds to a finite probability of dissociation up to infinite distances.

We have computed $\rho_1(\vec{r} - \vec{r}')$ along the nearest-neighbors (nn) direction which is ΓK in a hcp and $[111]$ in a bcc crystal. In Fig. 1 we report ρ_1 for a perfect hcp crystal at different densities at and above melting, and for a bcc crystal at $\rho = 0.02898 \text{\AA}^{-3}$. It is clear that at melting and at $\rho = 0.031 \text{\AA}^{-3}$, ρ_1 reaches a plateau at large distance whereas at $\rho = 0.033 \text{\AA}^{-3}$, ρ_1 steadily decreases with increasing distance. By averaging the tail in ρ_1 for distances greater than 14\AA , we find at the melting density a condensate fraction n_c

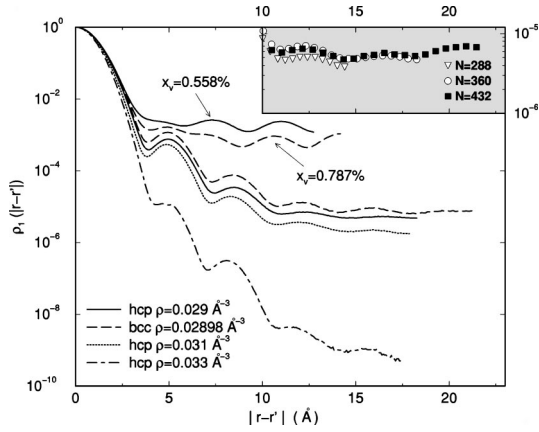


FIG. 1. $\rho_1(\vec{r}-\vec{r}')$ at different densities for hcp and bcc perfect ^4He crystals, and for the same crystals with a finite concentration x_v of vacancies.

$= (5.0 \pm 1.7) \times 10^{-6}$ in a perfect hcp and $(7.6 \pm 1.7) \times 10^{-6}$ in a perfect bcc crystal. This is a microscopic indication that BEC is present in perfect solid ^4He . (Ref. 19) At $\rho = 0.031 \text{ \AA}^{-3}$ we find $n_c = (2.0 \pm 0.4) \times 10^{-6}$ and at $\rho = 0.033 \text{ \AA}^{-3}$ the tail is so much depressed that the size of the simulation box is too small to conclude if ODLRO is present; in this case we can only say that the condensate fraction, if any, is lower than 10^{-9} . The simulation box which has been used to compute ρ_1 is cubic and contains $N = 432$ ^4He atoms for the bcc crystal, it is elongated in the ΓK direction, and contains $N = 360$ ^4He atoms for the hcp crystal. By changing the size of the boxes at fixed density we have checked that our results for ρ_1 have no finite-size effect within the statistical errors of our computations. This is shown in the inset of Fig. 1 for the hcp crystal at $\rho = 0.029 \text{ \AA}^{-3}$; by averaging the tail in ρ_1 for distances greater than 14 \AA , we find $n_c = (3.9 \pm 1.7) \times 10^{-6}$ for $N = 288$ and $n_c = (5.7 \pm 2.0) \times 10^{-6}$ for $N = 432$, to be compared with the value given above: $n_c = (5.0 \pm 1.7) \times 10^{-6}$ for $N = 360$. In Ref. 12 we found that a finite concentration of vacancies x_v induces a condensate fraction which depends linearly on x_v . In Fig. 1 we show also ρ_1 when a vacancy is present both in hcp (Ref. 12) and bcc. Taking into account the value of x_v of the computation we estimate that at $\rho = 0.029 \text{ \AA}^{-3}$ the condensate fraction due to a finite concentration of vacancies is equal to the one in a perfect hcp crystal when $x_v \approx 1.5 \times 10^{-5}$.

All the computed ρ_1 show oscillations which reflect the crystalline order in the system. However, these oscillations are not the same in the perfect and in the defected solid. We find that when a vacancy is present the maxima of the oscillations in ρ_1 correspond to multiples of the nn distance d_{nn} . This is an indication that in the presence of a vacancy the main mechanism which contributes to the separation of the two “half” particles is that one of them moves through the crystal following the vacancy which is very mobile.²⁰ The different positions of the maxima in ρ_1 for the perfect crystal suggest a different microscopic process for the ODLRO in this case. By analyzing the particle configurations sampled in our runs we find that the secondary peak of ρ_1 , located at about 5 \AA , always corresponds to a configuration in which the two “half” particles occupy two nn lattice positions

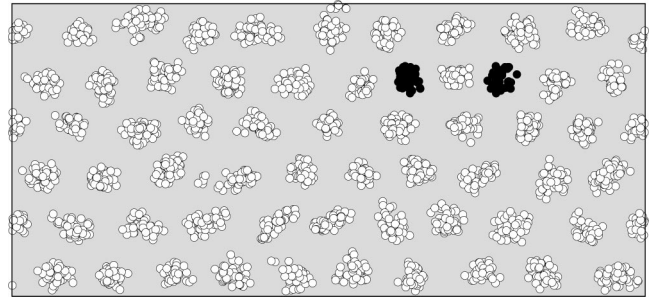


FIG. 2. Projection of 100 successive configurations of the particles (white circles) and the two “half” particles (black circles) in a basal plane of an hcp crystal at $\rho = 0.031 \text{ \AA}^{-3}$. ρ_1 is the probability distribution of the two “half” particles.

slightly distorted by the presence of one interstitial ^4He atom between them. In Fig. 2 we show 100 successive configurations of the particles which correspond to this event. In the formalism of second quantization $\rho_1(\vec{r}-\vec{r}')$ is equal to the expectation value of the composite event where one ^4He atom is destroyed at \vec{r}' and one is created at \vec{r} ; then it is possible to interpret the event in Fig. 2 as the creation of a VIP. The same process is found in a bcc crystal. After this first step the two “half” particles have a finite probability of moving away from one another by exchange processes with the other atoms, and this gives rise to the other maxima of ρ_1 at larger distance. By analyzing the particle configurations corresponding to these other maxima we find that a VIP is present in all the configurations. Similar processes were considered in Ref. 21 as a necessary condition for the supersolid phase, but there it is argued that VIP cannot be present. Our results disagree with this hypothesis. In order to characterize the anisotropy of ρ_1 as function of \vec{d} we have computed ρ_1 when the two “half” particles are no more constrained to lie in the nn direction but can freely move in a plane. In Fig. 3 one can see that ρ_1 in a perfect bcc crystal is strongly anisotropic for distances up to about 6 \AA , and the maxima of ρ_1 are in the direction of nn. However, at greater distances ρ_1 becomes nearly isotropic and we conclude that our estimation of the BEC fraction is not affected by the previous restriction on \vec{d} . Similar results are obtained for hcp. It is interesting to notice that when a vacancy is present the anisotropy of ρ_1 persists up to greater distances (data not

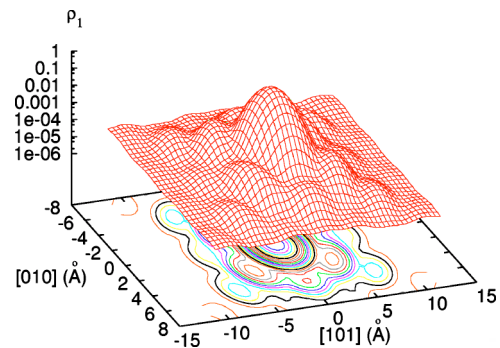


FIG. 3. (Color online) $\rho_1(\vec{r}-\vec{r}')$ at $\rho = 0.02898 \text{ \AA}^{-3}$ for a perfect bcc crystal with $\vec{r}-\vec{r}'$ lying in the plane $[-101]$.

shown). Also in Fig. 1 one can see that the oscillations of ρ_1 are more persistent with increasing distance in the crystal with a vacancy; this is another indication that different microscopic processes are at the origin of the ODLRO in the perfect and in the defected solid ^4He . The exchange of atoms and VIPs are present not only in ρ_1 but also in $|\Psi|^2$. At melting at about every 2×10^3 MC steps an atom has a displacement larger than d_m and in many cases this is associated with the presence of an interstitial. In principle one can devise an algorithm based on SPIGS to compute ρ_1 exactly. However, at present this appears to be a major computational problem. In any case we have given solid evidence that SWF overestimates the degree of local order so that we should expect that the SWF results for the BEC fraction are an underestimation of the exact values.

In conclusion we have shown that solid ^4He at $T=0$ K has BEC at melting density and above, at least up to 54 bars, whereas we find a vanishing BEC at 90 bars. Thus BEC should be at the basis of the NCRI observed experimentally.² Our result has been obtained from an advanced variational

theory, the accuracy of which has been tested with a projector method on the exact ground state. The key process giving rise to ODLRO is the formation of a VIP. Such defects have a finite probability to be present in the ground state of the system; they are not permanent excitations but simply rare fluctuations of the perfect crystal induced by the large zero-point motion. In other words, the number of atoms is equal to the number of lattice sites and, at the same time, atoms are delocalized. Since the ground state is the vacuum of the elementary excitations of the system we conjecture that a branch of low-energy excitations different from phonons should be present in solid ^4He . Such excitations should have an important role in determining the critical temperature. It is a possibility that this branch is related to some experimental results which have been interpreted in terms of an excitation with energy of about 2 K (Ref. 22).

This work was supported by the INFN Parallel Computing Initiative and by the Mathematics Department “F. Enriques” of the Università degli Studi di Milano.

¹E. Kim, and M. H. W. Chan, *Nature (London)* **427**, 225 (2004).

²E. Kim, and M. H. W. Chan, *Science* **305**, 1941 (2004).

³A. F. Andreev and I. M. Lifshitz, *Sov. Phys. JETP* **29**, 1107 (1969).

⁴G. V. Chester, *Phys. Rev. A* **2**, 256 (1970).

⁵F. Pederiva, G. V. Chester, S. Fantoni, and L. Reatto *Phys. Rev. B* **56**, 5909 (1997).

⁶D. E. Galli, L. Reatto, *J. Low Temp. Phys.* **134**, 121 (2004).

⁷A. J. Leggett, *Phys. Rev. Lett.* **25**, 1543 (1970); *J. Stat. Phys.* **93**, 927 (1998).

⁸M. Greiner, O. Mandel, T. Esslinger, T. W. Hansch, and I. Bloch, *Nature (London)* **415**, 39 (2002).

⁹J. F. Fernandez, and M. Puma, *J. Low Temp. Phys.* **17**, 131 (1974).

¹⁰W. M. Saslow, *Phys. Rev. Lett.* **36**, 1151 (1975).

¹¹W. M. Saslow, cond-mat/0407166 (unpublished).

¹²D. E. Galli and L. Reatto, *J. Low Temp. Phys.* **124**, 197 (2001).

¹³D. E. Galli and L. Reatto, *Mol. Phys.* **101**, 1697 (2003).

¹⁴A. Sarsa, K. E. Schmidt, and W. R. Magro, *J. Chem. Phys.* **113**,

1366 (2000).

¹⁵S. Vitiello, K. Runge, and M. H. Kalos, *Phys. Rev. Lett.* **60**, 1970 (1988).

¹⁶F. Pederiva, A. Ferrante, S. Fantoni, and L. Reatto *Phys. Rev. Lett.* **72**, 2589 (1994).

¹⁷R. A. Aziz, V. P. S. Nain, J. S. Carley, W. L. Taylor, and G. T. McConville, *J. Chem. Phys.* **70**, 4330 (1979); some tests with more recent forms for the interatomic potential give results similar to the present ones.

¹⁸This difference is reduced to 0.31 K with a fully optimized SWF [S. Moroni, D. E. Galli, S. Fantoni, and L. Reatto, *Phys. Rev. B* **58**, 909 (1998)]; but that optimization was performed only over a restricted density range so we have used the older form of SWF.

¹⁹In Ref. 12 we concluded that there was no BEC in the perfect solid; this was due to equilibration problems.

²⁰D. E. Galli and L. Reatto, *Phys. Rev. Lett.* **90**, 175301 (2003).

²¹N. Prokof'ev and B. Svistunov, cond-mat/0409472 (unpublished).

²²J. M. Goodkind, *Phys. Rev. Lett.* **89**, 095301 (2002).